The International Journal of Biochemistry & Cell Biology 74 (2016) 109–120

Contents lists available at ScienceDirect

The International Journal of Biochemistry & Cell Biology

journal homepage: www.elsevier.com/locate/biocel

Alterations of hemorheological parameters and tubulin content in erythrocytes from diabetic subjects

Ayelén D. Nigra, Noelia E. Monesterolo, Juan F. Rivelli, Marina R. Amaiden, Alexis N. Campetelli, Cesar H. Casale, Verónica S. Santander*

Departamento de Biología Molecular, Facultad de Ciencias Exactas, Físico-Químicas y Naturales, Universidad Nacional de Río Cuarto, Río Cuarto, 5800 Córdoba, Argentina

ARTICLE INFO

Article history:
Received 19 May 2015
Received in revised form 2 December 2015
Accepted 20 February 2016
Available online 26 February 2016

Keywords:
Tubulin
Diabetes
Erythrocyte deformability
Human erythrocytes
Acetylated tubulin
Osmotic fragility

ABSTRACT

Treatment of human erythrocytes with high glucose concentrations altered the content and distributions of three tubulin isotypes, with consequent reduction of erythrocyte deformability and osmotic resistance. In erythrocytes from diabetic subjects (D erythrocytes), (i) tubulin in the membrane-associated fraction (Mem-Tub) was increased and tubulin in the sedimentable fraction (Sed-Tub) was decreased, (ii) deformability was lower than in erythrocytes from normal subjects (N erythrocytes), and (iii) detyrosinated/acetylated tubulin content was higher in the Mem-Tub fraction and tyrosinated/acetylated tubulin content was higher in the Sed-Tub fraction, in comparison with N erythrocytes. Similar properties were observed for human N erythrocytes treated with high glucose concentrations, and for erythrocytes from rats with streptozotocin-induced diabetes. In N erythrocytes, high-glucose treatment caused translocation of tubulin from the Sed-Tub to Mem-Tub fraction, thereby reducing deformability and inducing acetylation/tyrosination in the Sed-Tub fraction. The increased tubulin acetylation in these cells resulted from inhibition of deacetylase enzymes. Increased tubulin acetylation and translocation of this acetylated tubulin to the Mem-Tub fraction were both correlated with reduced osmotic resistance. Our findings suggest that (i) high glucose concentrations promote tubulin acetylation and translocation of this tubulin to the membrane, and (ii) this tubulin is involved in regulation of erythrocyte deformability and osmotic fragility.

1. Introduction

In human erythrocytes, hyperglycemic stress induces imbalance of membrane lipids (Miller et al., 1980), alteration of membrane fluidity (Symeonidis et al., 2001), and reduced survival (Umudum et al., 2002). Human erythrocytes were long viewed as inert cells with limited or no ability to respond to external stimuli, and erythrocyte proteins were viewed as nonfunctional vestiges of precursor cells. However, studies in recent decades have revealed that human erythrocytes are highly responsive to environmental factors (Ferru et al., 2011; Foller et al., 2010; Kaestner et al., 2004; Olearczyk et al., 2004). Reports from numerous research groups have greatly increased our understanding of the structural organization and functions of erythrocytes, including detailed pathways whereby characteristic mechanical properties develop in normal erythrocytes and become defective in various disease processes (Mohandas and Gallagher, 2008).

Circulating mature erythrocytes in mammals differ from those in other vertebrate classes in that they lack nuclei. Nuclei are extruded from nucleated precursor cells in bone marrow during the final stages of erythroid maturation to yield reticulocytes, which then give rise to mature circulating erythrocytes. Mature erythrocytes in mammals also differ from those in other vertebrates in their shape and cytoskeletal composition (Koury et al., 1989). Erythrocytes of non-mammalian vertebrates have microtubules arranged in a subplasmalemmal ring in the equatorial plane, termed “the marginal band” (Granger et al., 1982). In contrast, mature mammalian erythrocytes do not contain microtubules (Cohen et al., 1990; Liao et al., 2000; Liu et al., 2010), although a few recent studies using proteomic technology demonstrated the presence of tubulin α6, β1, and α3 chains in human erythrocytes (Goodman et al.,

Abbreviations: N erythrocytes, erythrocytes from normal subjects; D erythrocytes, erythrocytes from diabetic subjects; Ac-Tub, acetylated tubulin; Sed-Tub, tubulin in sedimentable fraction; Mem-Tub, tubulin in membrane-associated fraction; Tyr-Tub, tyrosinated tubulin; Glu-Tub, detyrosinated tubulin; STZ, streptozotocin; NKA, Na^+,K^+-ATPase; TSA, trichostatin A.

* Corresponding author. Fax: +54 358 4676232.
E-mail address: vsantander@exa.unrc.edu.ar (V.S. Santander).

http://dx.doi.org/10.1016/j.biocel.2016.02.016
1357-2725/

2013). Previous studies by our group have revealed three distinct subcellular tubulin fractions in human erythrocytes: membrane-associated tubulin (Mem-Tub), cytosolic (soluble) tubulin, and a fraction sedimentable at 100,000 × *g* (Sed-Tub) (Amaiden et al., 2011). Tubulin is not a major protein by volume in erythrocytes, but it plays an important structural role and is involved in regulating the activity of crucial enzymes such as Na^+/K^+-ATPase (Amaiden et al., 2012, 2011) and PMCA (Monesterolo et al., 2008).

In our lab was previously determined that Mem-Tub content in erythrocytes and tissues containing insulin-insensitive glucose transporters from diabetic patients is higher than in normal subjects (Rivelli et al., 2012), and that translocation of tubulin from the Sed-Tub to Mem-Tub fraction is correlated with decreased erythrocyte deformability in humans and rats (Amaiden et al., 2012). In view of these findings, we hypothesized that exposure of erythrocytes to high glucose concentrations (as in diabetes) results in redistribution of tubulin among the subcellular fractions, with consequent alteration of hemorheological properties. In the present study, we examined the effects of various glucose concentrations on tubulin isotype levels, deformability, and osmotic fragility of erythrocytes.

2. Materials and methods

2.1. Materials

Nitrocellulose membrane, nocodazole, phenylmethylsulfonyl fluoride (PMSF), 4-chloro-1-naphthol, and sodium dodecyl sulfate (SDS) were from Sigma Chemical Co. (St. Louis, MO, USA). Lumigen™ PS-3 detection kit and high-performance chemiluminescence film were from GE Healthcare Life Sciences (Piscataway, NJ, USA).

2.2. Antibodies

Mouse mAb 6-11B-1 specific to acetylated tubulin (anti-Ac-Tub), mouse mAb DM1A specific to α-tubulin, mAb Tub1-A2 (anti-Tyr-Tub), peroxidase-conjugated mouse immunoglobulin G (IgG), peroxidase-conjugated rabbit IgG, fluorescein-conjugated mouse IgG, and fluorescein-conjugated rabbit IgG were from Sigma. Rabbit polyclonal antibody specific to detyrosinated tubulin (anti-Glu-Tub) was prepared in our laboratory as described by Gundersen et al. (1984).

2.3. Human subjects and erythrocyte preparation

Male and female patients (age 25–40 years) were recruited as blood donors at the Hospital Regional de Río Cuarto, Córdoba, Argentina. Patient selection and blood extraction were performed in compliance with relevant laws and institutional guidelines, using an informed consent protocol approved by the Committee on Research Ethics (CoEdi) of the Universidad Nacional de Río Cuarto, consistent with standards of Declaration of Helsinki.

Fresh blood samples were collected in Vacutainer tubes (Becton–Dickinson; Plymouth, UK), with ethylenediaminetetraacetic acid (EDTA; 1 mg/ml) as anticoagulant. Erythrocytes were obtained by conventional centrifugal separation and used immediately. Diabetic patients were selected by specific criteria, including blood glucose concentration >150 mg/dl. Venous blood samples were then analyzed for fasting glucose level by glucose oxidase method following 14-h fast. On another hand, hemoglobin A1C (HbA1C) level, which reflects glycosylation of the hemoglobin molecule, was measured to assess overall metabolic control during the preceding 8–12 weeks. Patient characteristics are summarized in Table 1. In some experiments, isolated erythrocytes were treated with 5 μM nocodazole, 10 μM taxol, 5 mM glucose, or 30 mM glucose for various durations as indicated in figure legends, and then washed twice in physiological saline.

Table 1
Clinical parameters of diabetic patients (D; $n = 20$) and normal subjects (N; $n = 20$) in this study.

Parameter	D	N
Age (years)	40 ± 15	43 ± 17
Sex (male/female)	12/8	9/11
Weight (kg)	66 ± 20	63 ± 15
HbA1C (%)	7 ± 0.5	*5 ± 0.2
Fasting plasma glucose (mg/dl)	135 ± 12	*80 ± 6
Diabetes type (I/II)	16/4	–
Fasting plasma insulin, (IU):		
<10	7	0
10–12	3	20
>12	10	0

HbA1C: glycosylation of hemoglobin molecule.
* $p < 0.05$.

2.4. Isolation of membrane, sedimentable, and cytosolic tubulin fractions from human erythrocytes

The following procedures were all performed at 4 °C. Two-ml blood samples were centrifuged, and serum and white blood cell layer were removed. Isolated erythrocytes were resuspended in 6 ml lysis buffer (7.5 mM sodium phosphate buffer, pH 7.5, containing 1 mM EDTA and 20 μg/ml PMSF) and incubated for 15 min at room temperature. The lysate was centrifuged (20,000 × *g*) for 20 min at 30 °C. The pellet was washed three times with 6 ml lysis buffer without PMSF, resuspended in 0.3 ml lysis buffer (Mem-Tub fraction), and stored at −20 °C until use. The supernatant fraction from the 20,000 × *g* centrifugation was immediately centrifuged at 100,000 × *g* for 30 min at 30 °C, and the pellet was resuspended in 0.3 ml lysis buffer (Sed-Tub fraction).

Erythrocytes were isolated by centrifugation (100 × *g*) of 2 ml treated or non-treated blood samples for 5 min. Serum and buffy coat fraction were discarded. Erythrocytes were resuspended in 6 ml lysis buffer on ice for 15 min and centrifuged at 100,000 × *g* for 1 h at 4 °C. Supernatant was recovered (cytosolic tubulin fraction) and used immediately.

2.5. Animals and in vivo experiments

Male Wistar rats of various ages were housed (five per cage) under conditions of controlled temperature and humidity, 12 h light/12 h dark cycle, and *ad lib* food and water. All experimental protocols followed guidelines in the Public Health Service Guide regarding care and use of laboratory animals, minimization of suffering, and number of animals used. Blood samples were obtained by tail vein puncture.

2.5.1. Induction of diabetes by streptozotocin (STZ) injection

Diabetes was induced by STZ treatment as described by Lin et al. (2005). In brief, 7-week-old rats were injected *i.p.* with a single dose of STZ (70 mg/kg, in citrate buffer 0.1 mM, pH 4.5). Control animals were injected with an equal volume of citrate buffer.

2.5.2. Glucose treatment

Adult rats (weight ~250 g) were fasted overnight and then injected *i.p.* with glucose (3600 mg/dl).

2.6. Rat brain tubulin preparation

Brains from 30- to 60-day-old rats were homogenized at 4 °C in 1 volume MEM buffer containing 1 mM $MgCl_2$. The homogenate was centrifuged at 100,000 × *g* for 45 min, and the pellet was discarded. Tubulin was purified by two cycles of assembly/disassembly followed by phosphocellulose chromatography (Sloboda and Rosenbaum, 1982).

2.7. Determination of acetylation capacity

Erythrocyte cytosolic fraction (100 μl) and purified rat brain tubulin (200 μg) were added to a reaction mixture (0.8 mM ethylene glycol tetraacetic acid [EGTA], 0.5 mM $MgSO_4$, 1 mM dithiothreitol [DTT]) in a final volume of 0.45 ml and incubated at 37 °C. At time points 0, 30, 60, and 90 min, a 100-μl aliquot was taken and α-tubulin and Ac-Tub contents were analyzed by immunoblotting. In control tubes, buffer solution was used instead of erythrocyte cytosolic fraction.

2.8. Immunofluorescence microscopy

Erythrocytes were fixed on coverslips with anhydrous methanol at −20 °C. Samples were washed, incubated with 2% (w/v) bovine serum albumin in phosphate-buffered saline (PBS) for 30 min, and stained by indirect immunofluorescence as described by DeWitt et al. (1998). The primary Abs used to visualize tubulin were: mAb DM1A (anti-α-tubulin; diluted 1:100), mAb 1A2 (anti-Tyr-Tub; diluted 1:100), polyclonal anti-Glu-Tub Ab (diluted 1:100), and mAb 6-11B-1 (anti-Ac-Tub; diluted 1:100). Fluorescein-conjugated anti-rabbit IgG (diluted 1:50) or anti-mouse IgG (diluted 1:50) were used as secondary Abs. Coverslips were mounted in Fluor-Save and observed by fluorescence microscopy (model H600L; Nikon; Tokyo, Japan).

2.9. Immunoblotting

Proteins were separated by SDS-PAGE on 12% polyacrylamide slab gel by Laemmli's method (Laemmli, 1970), and the gel was transferred to a nitrocellulose sheet. Blots were reacted with mAb DM1A (diluted 1:1000), mAb 6-11B-1 (diluted 1:1000), mAb 1A2 (diluted 1:1000), or polyclonal anti-Glu-Tub Ab (diluted 1:200). The sheet was reacted with peroxidase-conjugated corresponding anti-IgG Ab and stained using the 4-chloro-1-naphthol method or the ECL system. Band intensities were quantified using the Scion Image software program.

2.10. Determination of erythrocyte deformability

Erythrocyte deformability was measured according to the filtration method described by Cabrales (2007). In brief, polycarbonate filters (Nuclepore/Whatman; Pleasanton, CA, USA) (pore size 5 μm, diameter 13 mm, pore density $4 \times 103/mm^2$) were perfused with diluted cell suspensions using an infusion pump. Cell suspensions or medium (buffer) were delivered through the filter at rates of 0.5, 0.6, 0.7, 0.8, and 0.9 ml/min. Pressure drop across the filter was measured by a differential pressure transducer. Erythrocyte deformability was assessed by determination of the parameters β and ψ. β indicates resistance to flow through a filter pore calculated by the method of Skalak et al. (1983), based on the ratio of the initial pressure drop across the filter (with cells present) to the pressure drop with buffer alone:

$$\beta = \left(\frac{Pi}{Po} - 1\right)\frac{\upsilon}{h} + 1$$

Pi = pressure drop across filter; Po = pressure drop in presence of cells; υ = ratio of mean cell volume to pore volume; h = volume packed erythrocyte fraction of the perfusate. Filtration measurements were performed in triplicate at hematocrit 0.12, using different filters, and averaged. The value of β depends on the flow used to deform the cells. ψ indicates the slope of the curve β *vs.* flow.

2.11. Determination of erythrocyte osmotic fragility

Whole blood anticoagulated with EDTA (10 μl) was added to 1 ml of various saline solutions (NaCl concentrations 0.3, 0.35, 0.4, 0.45, 0.5, 0.55, 0.6, 0.65, 0.7, 0.75, 0.8, and 0.9%). Samples were incubated for 15 min at room temperature and centrifuged for 5 min at 100 × *g*. Hemoglobin in each supernatant was quantified by spectrophotometry at wavelength 540 nm, and this value was converted to percent hemolysis with the extreme NaCl concentrations (0.3% and 0.9%) considered as full-lysis control and blank, respectively. Percent hemolysis was plotted against saline concentration, and median corpuscular fragility (MCF), *i.e.*, the saline concentration causing 50% hemolysis, was determined (Behling-Kelly and Collins-Cronkright, 2014).

2.12. Protein concentration

Protein concentration was determined by the method of Bradford (1976).

2.13. Statistical analysis

Results were expressed as mean ± SD. Student's *t*-test was used for comparison of two groups. Differences in means were considered statistically significant for $p < 0.05$.

3. Results

3.1. Diabetes mellitus induces modification of tubulin distribution and deformability in erythrocytes

Plasma membrane Na^+/K^+-ATPase (NKA) activity in erythrocytes is lower for diabetic subjects than for normal subjects (Rivelli et al., 2012; Kumar, 2012; Rabini et al., 1997). Our previous report showed that such reduction is correlated with increased content of Mem-Tub and Ac-Tub/NKA complex (Rivelli et al., 2012), and that tubulin in human erythrocytes is distributed in three subfractions (membrane, cytosolic, and sedimentable) (Amaiden et al., 2011). To test the hypothesis that this distribution is altered in erythrocytes from diabetic subjects (hereafter termed "D erythrocytes" for convenience) and affects NKA activity, tubulin distribution in D erythrocytes and in erythrocytes from normal subjects (hereafter termed "N erythrocytes") was determined by indirect immunofluorescence using anti-α-tubulin mAb DM1A. There was a clear difference in tubulin distribution (Fig. 1A, left panels). In D erythrocytes, fluorescence was observed on the entire cell surface, indicating that tubulin was localized in the membrane (Mem-Tub). In N erythrocytes, fluorescence was observed as a ring, a typical pattern for Sed-Tub (Amaiden et al., 2011). These observations were confirmed by quantification of inner fluorescence along the erythrocyte diameter (Fig. 1A, right panels). Immunoblotting analysis gave similar results. In N erythrocytes, content of Sed-Tub was ~4× higher than that of Mem-Tub, whereas in D erythrocytes content of Mem-Tub was higher than that of Sed-Tub (Fig. 1B).

Our 2012 study showed that increased Mem-Tub is related to decreased erythrocyte deformability (Amaiden et al., 2012). Because Mem-Tub content was higher in D erythrocytes, deformability of these cells was investigated. ψ value was ~30% higher in

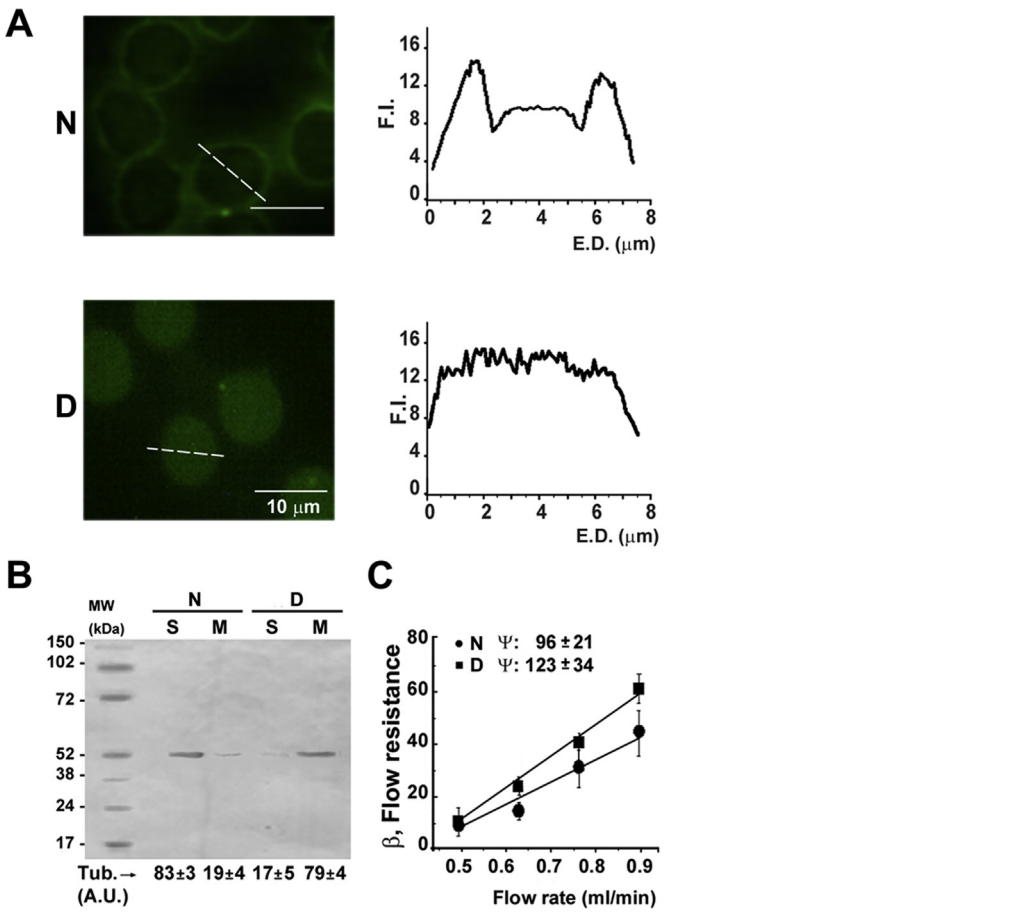

Fig. 1. Tubulin distribution and deformability of D erythrocytes. (A) Human diabetic (D) and normal (N) erythrocytes were fixed on coverslips and analyzed by immunofluorescence microscopy using anti-α-tubulin mouse mAb DM1A. Inner immunofluorescence was measured along the white dashed line using the Scion Image software program. Curves in right panels: *y*-axis = fluorescence intensity (F.I.); *x*-axis = erythrocyte diameter (E.D.); bar = 10 μm. (B) Sed-Tub (S) and Mem-Tub (M) fractions were obtained from 2 ml human blood as described in M&M. An aliquot of each fraction was used for determination of α-tubulin amount by immunoblotting with mAb DM1A. Volumes loaded on each well were calculated to be representative of equivalent amounts of erythrocytes. Experiments were performed in triplicate, and a representative blot is shown. Tubulin bands were quantified using the Scion Image program, and values were expressed as arbitrary units (mean ± SD from three independent experiments). (C) Flow resistance (β) through a filter pore was determined for D and N erythrocytes, as described in M&M. Deformability (ψ) values were calculated from the slope of the curve. β and ψ values shown are mean ± SD from three independent experiments.

D erythrocytes than in N erythrocytes (Fig. 1C), indicating reduced deformability. This finding suggests that tubulin in D erythrocytes is translocated from the Sed-Tub to the Mem-Tub fraction with consequent decrease of deformability, as observed previously in erythrocytes from hypertensive subjects (Amaiden et al., 2012).

To test whether diabetes development causes tubulin redistribution, erythrocyte tubulin distribution in an STZ-induced diabetic rat model was analyzed by indirect immunofluorescence. Matched control animals were injected with citrate buffer (the STZ vehicle). Blood was sampled immediately after STZ or vehicle administration for evaluation of glycemia and erythrocyte tubulin distribution. At this time point (day 0), tubulin in both groups was localized in the Sed-Tub fraction (Fig. 2A). In the STZ-treated group, glycemia values were increased 85% and 225% at days 4 and 6, in association with translocation of tubulin from the Sed-Tub to Mem-Tub fraction (Fig. 2A). These findings were consistent with quantification of inner fluorescence along the erythrocyte diameter (Fig. 2B). In the control group, glycemia values and tubulin distribution pattern did not show notable time-dependent changes. The increase in Mem-Tub content in the STZ-treated group was associated with a ~70% increase in Ψ value, indicating reduced erythrocyte deformability (Fig. 2C), similar to results for human erythrocytes.

3.2. Hyperglycemia alters tubulin distribution and deformability

Hyperglycemia is a typical sign of diabetes, and may be responsible for alterations of tubulin distribution and deformability in D erythrocytes. To test this possibility, tubulin distribution was examined in *in vitro* human erythrocytes exposed to high glucose levels. Erythrocytes were incubated with 30 mM glucose (equivalent to 540 mg/dl) for 2 h at 37 °C to simulate diabetic hyperglycemia. Control erythrocytes were incubated with 5 mM glucose (equivalent to 90 mg/dl, the normal level). Tubulin distribution was analyzed by indirect immunofluorescence. High-glucose treatment had no effect on tubulin content (as indicated by fluorescence intensity quantification; data not shown), but did alter tubulin distribution (Fig. 3A, left panels). Fluorescence in the experimental group was observed over the entire cell surface (Mem-Tub localization), but that in the control group appeared as a ring underneath the membrane (Sed-Tub localization). These findings were consistent with quantification of inner fluorescence along the erythrocyte diameter (Fig. 3A, right panels). Immunoblotting analysis of tubulin content in the experimental group showed a ~70% decrease in the Sed-Tub fraction and a ~140% increase in the Mem-Tub fraction (Fig. 3B). Thus, high-glucose treatment induced translocation of tubulin from the Sed-Tub to the Mem-Tub fraction, similar to results for D erythrocytes (Fig. 1). Translocation to the Mem-Tub

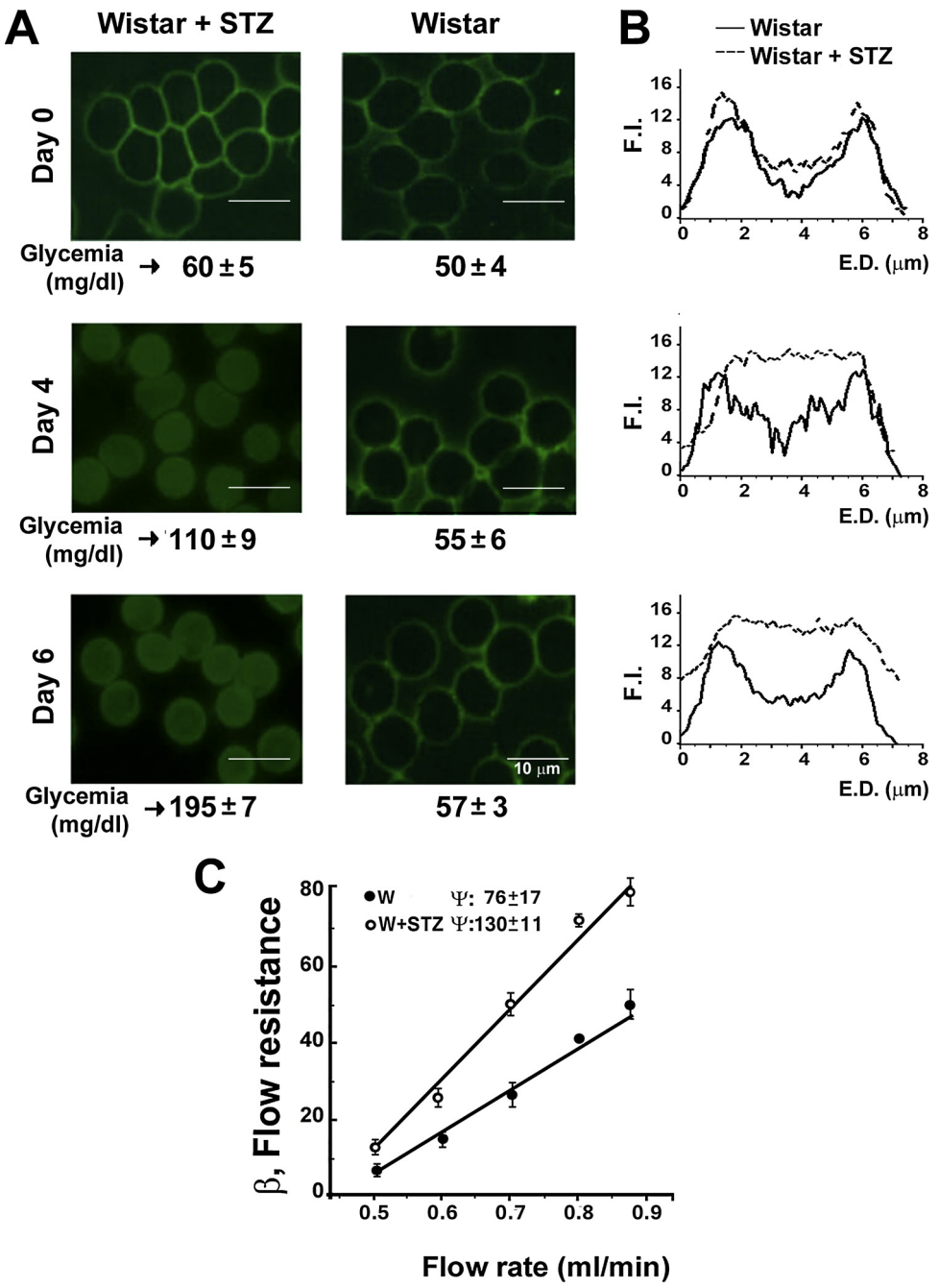

Fig. 2. Tubulin distribution in erythrocytes of rats with STZ-induced diabetes. Wistar rats were injected with a single dose of STZ (70 mg/kg, in 0.1 mM citrate buffer, pH 4.5). Control animals were injected with an equal volume of citrate buffer. Blood aliquots were taken at 0, 4, and 6 days. (A) Erythrocytes from the two groups were fixed on coverslips and analyzed by immunofluorescence microscopy using mAb DM1A. Glycemia value (mg/dl glucose in blood) was measured. Bar = 10 μm. (B) Inner immunofluorescence was measured and expressed as in Fig. 1A. (C) Flow resistance (β) of erythrocytes from the two groups at day 4 was determined, ψ values were calculated, and β and ψ values are expressed as in Fig. 1C.

fraction was associated with reduced erythrocyte deformability; Ψ value was increased ~30% in the experimental group (Fig. 3C).

The effect of glucose was concentration-dependent. A small amount of tubulin was present in membranes of erythrocytes treated with 20 mM glucose, but translocation was greatly increased at glucose concentrations ≥30 mM (Suppl. Fig. S1). In association with such tubulin translocation, erythrocyte deformability was also affected by glucose treatment in a dose-dependent manner, as observed for glucose concentrations ≥20 mM. Taken together, these findings indicate that exposure of erythrocytes to high glucose concentrations results in redistribution of tubulin from the Sed-Tub to the Mem-Tub fraction and a consequent decrease in deformability.

For *in vivo* evaluation of glucose effect, overnight-fasted rats were injected *i.p.* with glucose, while control animals were injected with physiological saline. Blood samples were taken at various time points for measurement of glycemia, erythrocyte tubulin distribution, and deformability. In the experimental group, blood glucose concentration was ~40% higher at 45 min than at 0 min (Fig. 4A). Tubulin was localized in the Sed-Tub fraction at 0 min, but was translocated to the Mem-Tub fraction by 45 min, in association with a peak in glycemia (Fig. 4A and B). By 75 min, glycemia returned to basal levels and tubulin returned to the Sed-Tub fraction (Fig. 4A

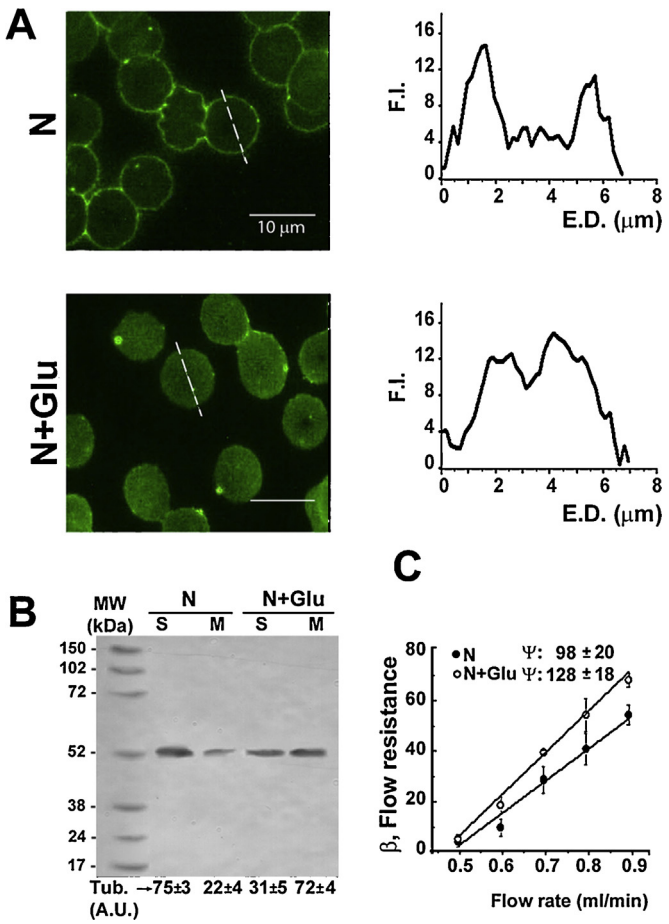

Fig. 3. Effects of glucose on erythrocyte tubulin distribution and deformability. Human erythrocytes were incubated for 2 h with 5 mM (control) or 30 mM glucose. (A) Erythrocytes were fixed on coverslips and analyzed by immunofluorescence microscopy using mAb DM1A. Inner immunofluorescence was measured and expressed as in Fig. 1A. Bar = 10 μm. (B) Sed-Tub (S) and Mem-Tub (M) fractions were obtained, α-tubulin amounts were determined, and tubulin bands were quantified as described in Fig. 1B. (C) Flow resistance (β) of erythrocytes from the two groups was determined, ψ values were calculated, and β and ψ values are expressed as in Fig. 1C.

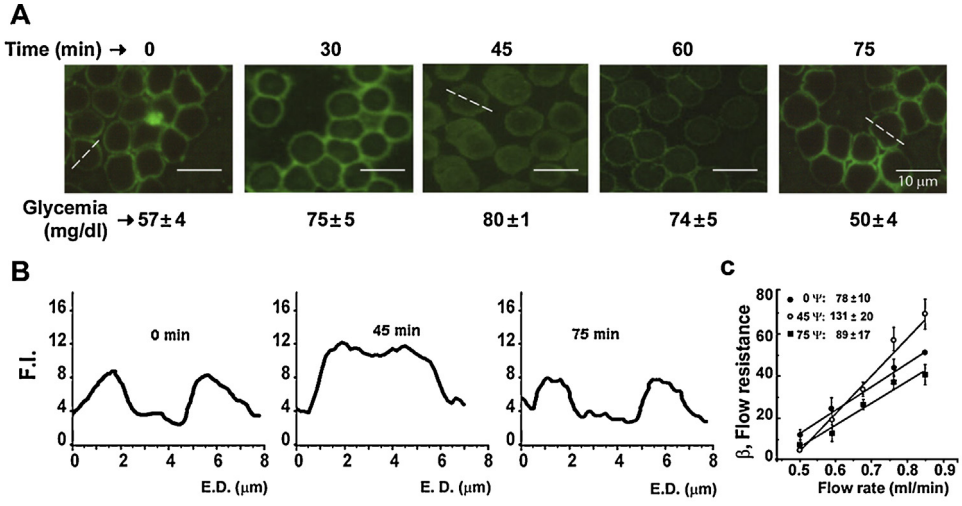

Fig. 4. *In vivo* effects of glucose treatment on tubulin distribution and deformability of rat erythrocytes. Wistar rats were injected with 30 mM glucose. Blood aliquots were taken at 0 min, 30 min, 45 min (when glycemia was maximal), 60 min, and 75 min (when glycemia returned to basal value). (A) Erythrocytes were fixed on coverslips and analyzed by immunofluorescence microscopy using mAb DM1A. Bar = 10 μm. (B) Inner immunofluorescence was measured and expressed as in Fig. 1A. (C) Flow resistance (β) of erythrocytes was determined, ψ values were calculated, and β and ψ values are expressed as in Fig. 1C.

and B), indicating that the effect of glucose is reversible. Erythrocyte deformability was inversely correlated with Mem-Tub content. At 45 min, when glycemia and Mem-Tub content were elevated, Ψ value was ~70% higher than at 0 min, indicating reduced deformability. At 75 min, when glycemia and tubulin distribution had returned to basal levels, Ψ value was similar to that of the

control group (Fig. 4C). At 0 min, glycemia values were similar (~60 mg/dl) and tubulin was localized in the Sed-Tub fraction for the two groups. The above parameters were not affected by administration of physiological saline (data not shown).

3.3. High-glucose treatment and diabetes alter content and distribution of acetylated, tyrosinated, and detyrosinated tubulin isotypes

Our previous studies showed that various environmental conditions affect content and distribution of the three major tubulin isotypes (Ac-Tub, Tyr-Tub, Glu-Tub) in erythrocyte membranes (Amaiden et al., 2012; Rivelli et al., 2012). In the present study, specific Abs and immunofluorescence microscopy were used to analyze distribution of these three isotypes in human N and D erythrocytes. D erythrocytes displayed fluorescence over the entire cell surface, indicating increased levels of all three isotypes in the membrane (Fig. 5A), consistently with immunoblotting results in our 2012 study (Rivelli et al., 2012).

If the observed changes in Mem-Tub isotype in D erythrocytes are mediated by translocation of tubulin from the Sed-Tub fraction, it is possible that tubulin isotypes in the Sed-Tub fraction are also modified. To test this possibility, tubulin isotypes in Sed-Tub fractions from D and N erythrocytes were analyzed. Total tubulin in this fraction was ~80% lower in D than in N erythrocytes (Fig. 5B), supporting the translocation hypothesis. Tubulin remaining in the Sed-Tub fraction of D erythrocytes was highly acetylated; *i.e.*, the ratio of Ac-Tub to α-tubulin was ~7, whereas the corresponding ratio for N erythrocytes was ~0.3 (Fig. 5B). A similar relationship, but with lesser degree, was observed for Tyr-Tub. The ratio of Tyr-Tub to α-tubulin content in Sed-Tub fraction was ~3.6 for D erythrocytes, but only ~0.4 for N erythrocytes (Fig. 5B). The pattern for Glu-Tub in D erythrocytes was similar to that for α-tubulin; there was a significant decrease in the Sed-Tub fraction at levels that were not detectable by western blotting (Fig. 5B).

Hyperglycemia is a typical sign of diabetes, and may be involved in alteration of tubulin isotypes in D erythrocytes. High-glucose treatment of N erythrocytes produced changes in α-tubulin distribution similar to those observed in D erythrocytes. Indirect immunofluorescence showed that total tubulin was translocated from the Sed-Tub to Mem-Tub fraction in treated cells (Fig. 5A). Ac-Tub was increased in the Mem-Tub and Sed-Tub fractions of glucose-treated N erythrocytes, reaching levels similar to those in D erythrocytes (Fig. 5A). Distribution of Glu-Tub was similar to that of α-tubulin; glucose treatment resulted in translocation to the Mem-Tub fraction (Fig. 5A). Overall fluorescence corresponding to Tyr-Tub was reduced in treated cells, but the distribution of this isotype was unchanged (Fig. 5A).

Consistent with the above findings, immunoblotting analysis showed $\alpha > 50\%$ reduction of α-tubulin and Glu-Tub in the Sed-Tub fraction of glucose-treated N erythrocytes (Fig. 5B). In contrast, Ac-Tub content of this fraction increased >100% in treated cells. Tyr-Tub content in the Sed-Tub fraction was slightly reduced in treated cells; however, the ratio of Tyr-Tub to α-tubulin increased ~40% because Tyr-Tub was not translocated to the membrane (Fig. 5B). Taken together, these findings indicate that high-glucose treatment of human erythrocytes induces acetylation of tubulin and translocation of tubulin (particularly Ac-Tub and Glu-Tub isotypes) from the Sed-Tub to the Mem-Tub fraction.

3.4. Glucose treatment reduces deacetylation capacity

The observed increase of Ac-Tub level resulting from high-glucose treatment suggested an alteration of acetylation/deacetylation equilibrium. To evaluate this possibility, acetylation/deacetylation capacity was examined under various conditions. Rat brain tubulin was incubated for various durations with cytosolic fractions from D erythrocytes, N erythrocytes, and N erythrocytes pretreated with 30 mM glucose, and tubulin acetylation levels were measured. For non-treated N erythrocytes, acetylation level declined in a time-dependent manner. Relative to the value at 0 min, acetylation was reduced ~50% at 30 min and reached its minimal value (~20% of baseline) at 90 min (Fig. 7A and B). Acetylation was also reduced, but to a lesser degree, for D erythrocytes and glucose-treated N erythrocytes. For these two groups, the reduction was statistically significant at 60 min, and the minimal values were respectively ~60% and ~70% of baseline (Fig. 6A and B). These findings suggest that N erythrocytes have high deacetylase activity, and that this activity is inhibited by glucose. When the above experiments were performed with non-treated N erythrocytes in the presence of trichostatin A (TSA), an inhibitor of HDAC6 (the enzyme responsible for tubulin deacetylation), results were similar to those for D erythrocytes and glucose-treated N erythrocytes (Fig. 6A and B).

3.5. High-glucose treatment and tubulin acetylation alter osmotic fragility

High-glucose treatment resulted in increased Mem-Tub content and reduced erythrocyte deformability. We therefore evaluated effects of high-glucose treatment on osmotic fragility, a parameter that reflects resistance to osmotic stress. Visual inspection of test tubes indicated clearly that D erythrocytes were more sensitive to hemolysis than were N erythrocytes; *i.e.*, hemolysis was detected for all tested NaCl concentrations in the former group, but only for NaCl concentrations ≤0.5% in the latter group (Fig. 7A). Fig. 7B is an osmotic fragility curve with hemolysis percentage shown as a function of extracellular osmolarity (NaCl in suspension medium). The rightward shift seen for D erythrocytes indicates greater susceptibility to reduced osmotic pressure; *i.e.*, these cells undergo lysis following a smaller reduction in NaCl concentration in comparison with N erythrocytes. Values of MCF were $0.61 \pm 0.03\%$ for D erythrocytes and $0.43 \pm 0.01\%$ for N erythrocytes. Resistance to osmotic stress declined as a function of time for N erythrocytes treated with 30 mM glucose; MCF values were $0.53 \pm 0.03\%$ at 2 h, $0.57 \pm 0.01\%$ at 3 h, and $0.65 \pm 0.05\%$ at 7 h (Fig. 7C). Resistance to osmotic stress also varied as a function of glucose concentration applied (Suppl. Fig. S1C).

Taxol and nocodazole, two drugs that affect dynamic properties of microtubules, modify tubulin content in both Mem-Tub and Sed-Tub fractions; taxol causes association whereas nocodazole causes dissociation of tubulin (Amaiden et al., 2011). We evaluated effects of these two drugs on glucose-induced osmotic fragility. In erythrocytes pretreated with 10 μM taxol for 4 h, glucose treatment did not reduce fragility (Fig. 7D), suggesting that the effect of glucose requires dissociation of tubulin in both the Sed-Tub and Mem-Tub fractions. In cells pretreated with 50 μM nocodazole for 4 h to dissociate tubulin, the effect of glucose was not reversed. These findings, taken together, indicate that the effect of glucose is mediated by dissociation rather than association of tubulin in the two fractions.

Because glucose induces hyperacetylation of tubulin (Fig. 2), it is possible that both translocation to the Mem-Tub fraction and hyperacetylation are involved in reduction of osmotic fragility. To evaluate this possibility, osmotic fragility was examined in the presence of TSA. TSA-treated cells were more susceptible to reduced osmotic pressure; *i.e.*, MCF was $0.51 \pm 0.001\%$ in treated cells and $0.43 \pm 0.01\%$ in non-treated cells (Fig. 7D). The effect of glucose was more pronounced in cells co-incubated with TSA and glucose for 3 h; MCF was $0.60 \pm 0.005\%$, similar to the value ($0.65 \pm 0.05\%$) for cells treated with glucose for 7 h (Fig. 7C and D). These findings suggest that glucose inhibits deacetylase activity

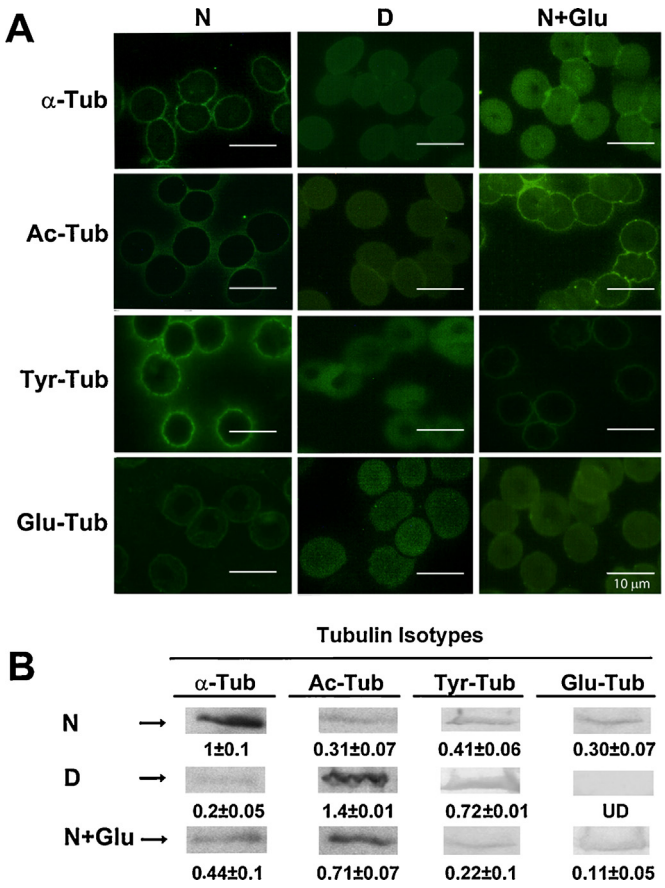

Fig. 5. Distribution of tubulin isotypes. Non-treated N erythrocytes (N), D erythrocytes (D), and N erythrocytes incubated with 30 mM glucose for 2 h (N + Glu) were analyzed. (A) Erythrocytes were fixed on coverslips and analyzed by immunofluorescence microscopy using anti-α-tubulin mAb DM1A, anti-Ac-Tub mAb 6-11B-1, anti-Glu-Tub rabbit polyclonal Ab, and anti-Tyr-Tub mAb 1A2. Bar = 10 μm. (B) Sed-Tub fraction was obtained, amounts of α-tubulin and the three tubulin isotypes were determined, and tubulin bands were quantified as described in Fig. 1B. UD: undetected.

and consequently increases Ac-Tub content, and that these changes are involved in alteration of osmotic fragility.

4. Discussion

Our previous studies showed that tubulin in human erythrocytes is distributed in three operationally distinguishable pools: membrane, cytosolic, and sedimentable fractions (Amaiden et al., 2011). Results of the present study indicate that such distribution is altered in D erythrocytes, and that the alteration is due to elevated glucose concentration, which induces translocation of tubulin from the Sed-Tub to Mem-Tub fraction. This conclusion is based on two observations: (i) Tubulin is localized primarily in the Mem-Tub fraction in D erythrocytes, and in the Sed-Tub fraction in N erythrocytes. Induction of diabetes in N erythrocytes by STZ treatment resulted in translocation of tubulin from the Sed-Tub to Mem-Tub fraction. (ii) Redistribution of tubulin from the Sed-Tub to Mem-Tub fraction was also observed in high-glucose-treated human erythrocytes and erythrocytes of hyperglycemic rats. These findings suggest that high glucose concentration activates a mechanism leading to migration of tubulin to the membrane, similar to our previous observations in COS and CAD cells (Rivelli et al., 2012).

Although the mechanism of tubulin migration remains unclear, it appears that tubulin must be acetylated in order to migrate to the membrane (Santander et al., 2006; Zampar et al., 2009). In the present study, glucose not only induced translocation of tubulin to the membrane, but also affected the balance among three tubulin isotypes, particularly in regard to acetylation, which was apparently promoted by glucose-mediated inhibition of deacetylation. In D erythrocytes and glucose-treated N erythrocytes, increased total tubulin content in the Mem-Tub fraction was due mainly to the Ac-Tub and Glu-Tub isotypes. Tubulin remaining in the Sed-Tub fraction was hyperacetylated. Cytosolic extracts of D erythrocytes and glucose-treated N erythrocytes inhibited tubulin deacetylation *in vitro*, similarly to TSA.

Protein acetylation is an important posttranslational modification involved in the regulation of numerous cellular events (Kouzarides, 2000; Polevoda and Sherman, 2002; Xiong and Guan, 2012), including cell response to high glucose concentration (Kosanam et al., 2014; Lin et al., 2014; Liu et al., 2014; Zhao et al., 2010). Zhao et al. (2010) reported that lysine acetylation is a frequently occurring modification in enzymes that catalyze intermediate metabolism, and modulates metabolic pathways that involve those enzymes. Glucose-mediated protein acetylation is due to inhibition of deacetylases such as histone deacetylases (Lin et al., 2014) and sirtuins (Chalkiadaki and Guarente, 2012). In the present study, high glucose concentrations altered acetylation/deacetylation equilibrium in cells with high deacetylase activity, suggesting that high glucose inhibits deacetylase activity and consequently promotes tubulin acetylation. This process appears to function as a signal for glucose to promote migration of tubulin to the erythrocyte membrane. Experiments to test this hypothesis are underway.

Migration of Ac-Tub to the membrane triggers various physiological events that affect both enzyme activities and rheological properties of the membrane. A series of our previous studies demonstrated that Ac-Tub forms complexes with NKA, PMA1, and PMCA, leading to inhibition of membrane enzyme activity both

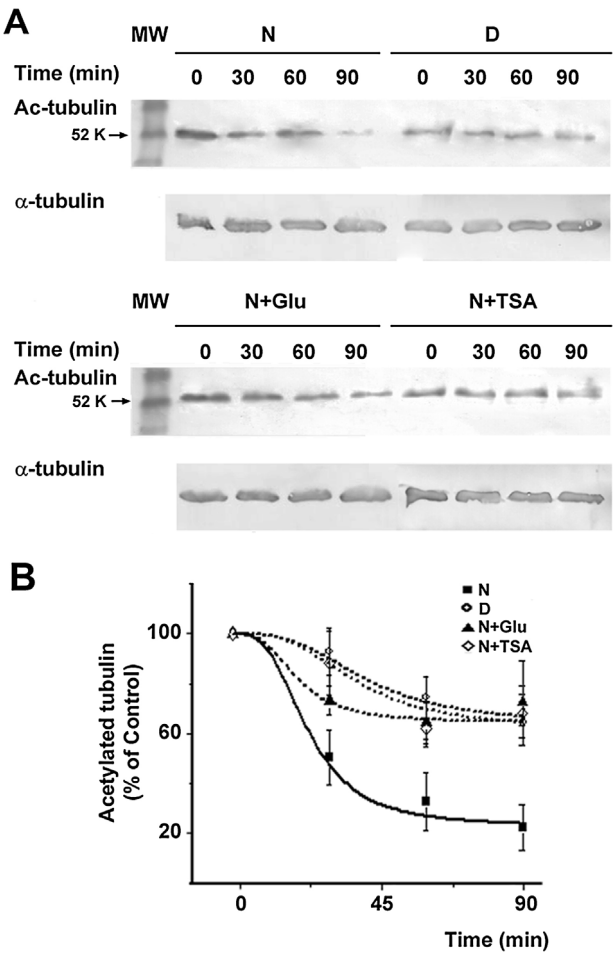

Fig. 6. Acetylation capacity of erythrocytes. Acetylation capacity was determined for cytosolic fractions from N erythrocytes, D erythrocytes, N erythrocytes treated with 30 mM glucose for 3 h, and N erythrocytes treated with 5 μM TSA for 6 h. Fractions were incubated with rat brain tubulin as described in M&M, aliquots were taken at the indicated times, and α-tubulin and Ac-Tub contents were determined by immunoblotting with mAbs DM1A and 6-11B-1. (A) Representative blot from three independent experiments, with α-tubulin (mAb DM1A) as loading control. (B) Bands were quantified using the Scion Image program, and values (expressed as percentages of value at 0 min) were plotted as a function of incubation time. Values shown (mean ± SD) are from three independent experiments.

in vivo and *in vitro* (Campetelli et al., 2013, 2005; Casale et al., 2005, 2003, 2001; Monesterolo et al., 2008; Santander et al., 2006; Zampar et al., 2009). We showed recently that the tubulin detyrosination/tyrosination cycle is involved in regulation of NKA activity, and that detyrosinated Mem-Tub enhances the inhibitory effect of Ac-Tub on NKA activity (Amaiden et al., 2015). The present findings indicate that membrane Glu-Tub level is increased in D erythrocytes and glucose-treated N erythrocytes. Such increase may also be involved in regulation of NKA activity.

Increased levels of membrane Ac-Tub promoted erythrocyte deformability and osmotic fragility. In contrast, increased Mem-Tub levels in human and rat erythrocytes resulted in reduced deformability in our previous studies (Amaiden et al., 2012, 2011). Associations among high glucose level, Mem-Tub content, osmotic fragility, and deformability were observed in the present study. It is too soon to conclude that Mem-Tub accumulation is the molecular cause of reduced deformability; however, it is noteworthy that values of the deformability parameter Ψ in human and rat erythrocytes are altered by changes in Mem-Tub content induced by high-glucose treatment or diabetes. Increased Mem-Tub content was associated with higher Ψ value and consequently lower deformability (Figs. 1–4C). The same phenomenon was observed in erythrocytes from hypertensive subjects (Amaiden et al., 2012). Reduced deformability in D erythrocytes and glucose-treated N erythrocytes has been reported by many other groups (Berndt-Zipfel et al., 2013; Manno et al., 2010; Richards and Nwose, 2010; Schwartz et al., 1991; Shin et al., 2007). Erythrocyte deformability is generally believed to be determined primarily by geometric factors such as corpuscular volume and shape and internal viscosity (as reflected by hemoglobin content), and by membrane properties (Ariyoshi et al., 2012). Ballas et al. (1984) concluded that reduced deformability resulted from alterations in membrane lipid composition, NKA enzyme activity, and/or Na^+/K^+ uptake. On the other hand, Gyawali et al. (2012) proposed that membrane proteins (*e.g.*, spectrin, ankyrin, protein 4.2) are more heavily glycosylated in D erythrocytes than in N erythrocytes, and that reduced deformability results from glycosylation-mediated oxidative modification of spectrin.

The present findings indicate that reduced erythrocyte deformability results from increased tubulin content in membrane fractions; however, involvement of other factors cannot be ruled out. In diabetes, increased levels of membrane tubulin result from elevated glucose concentrations. It is possible that reduced erythrocyte deformability in other pathological states is associated with changes in tubulin content in membranes. Our recent study showed that increased membrane tubulin content in hypertensive subjects altered erythrocyte deformability. In this case, elevation of membrane tubulin involved changes in the tubulin tyrosination/detyrosination cycle (Amaiden et al., 2015). Reduced erythrocyte deformability has been reported in dyslipidemia

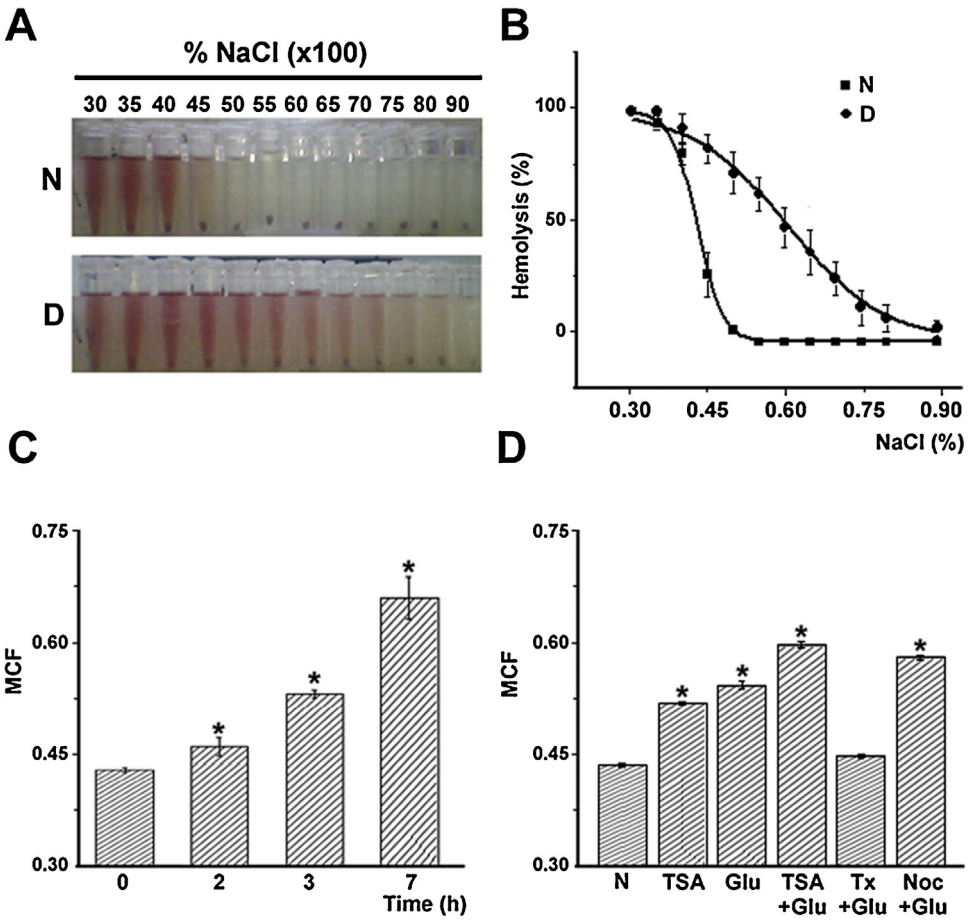

Fig. 7. Osmotic fragility of erythrocytes under various NaCl concentrations. Osmotic fragility of N and D erythrocytes was measured as a percentage of hemolysis of erythrocytes incubated in various NaCl concentrations. (A) Representative images of hemolysis tubes from eight independent experiments. (B) Hemolysis percentage values for N and D erythrocytes were calculated and plotted as a function of NaCl concentration. Values shown are mean ± SD from eight independent experiments. (C) Median corpuscular fragility (MCF; *i.e.*, NaCl concentration causing 50% hemolysis) was calculated for N erythrocytes treated with 30 mM glucose for 0, 2, 3, or 7 h. (D) MCF values were calculated for non-treated N erythrocytes (N), and for N erythrocytes treated with 30 mM glucose for 3 h (Glu), TSA for 6 h (TSA), both TSA and glucose (TSA + Glu), 5 μM taxol for 4 h (Tx + Glu), or 50 μM nocodazole for 4 h and 30 mM glucose for 3 h (Noc + Glu).

patients (Uydu et al., 2012; Karbiner et al., 2013). In the present study, differences were observed in lipid content between N and D erythrocytes (Table 1). However, differential changes in erythrocyte deformability in response to high glucose were observed in samples with similar lipid content, suggesting that the glucose effect is independent of lipid content (Figs. 3 and 4). On the other hand, we observed recently that diacylglycerol (DAG) treatment of human erythrocytes increased membrane tubulin content (Monesterolo et al., 2015). These findings, taken together, suggest that altered lipid content in dyslipidemia patients may not be the direct cause of reduced erythrocyte deformability, but the two processes may be related. Studies to clarify this point are underway.

Membrane Ac-Tub level is clearly related to osmotic fragility of erythrocytes. In the present study, the fragility curve was sigmoidal (S-shaped) for N erythrocytes but nearly linear for D erythrocytes. Hamidi et al. (2001) reported similar findings for drug-loaded erythrocytes. The D erythrocyte population is evidently more heterogeneous than the N erythrocyte population in terms of membrane resistance to changes in external osmotic pressure. Increased erythrocyte osmotic fragility has been observed in several studies of metabolic syndrome (which includes hypertension and diabetes), and such increase is associated with change in fragility curve shape from sigmoidal to more linear. Besides increased osmotic fragility, metabolic syndrome often involves morphological transformation and consequent reduction of erythrocyte deformability and membrane fluidity (Gyawali and Richards, 2015; Gyawali et al., 2014). In the present study, a correlation between degree of resistance to osmotic stress and duration of glucose treatment was observed. Osmotic fragility was promoted by tubulin acetylation and increased dissociation ability of Sed-Tub and Mem-Tub fractions; *i.e.*, TSA treatment of erythrocytes increased MCF, and taxol treatment abolished the effect of glucose on fragility. We cannot rule out the possibility that resistance to osmotic stress also involves factors involved in translational modification of proteins, *e.g.*, phosphorylation.

Tubulin in erythrocytes evidently exists in a balance between the Sed-Tub and Mem-Tub fractions. This balance can be modified depending on the needs of the cell, resulting in both mechanical (deformability, osmotic fragility) and physiological changes (ion transport, modified enzyme activity of NKA and PMCA). Our knowledge of the Mem-Tub fraction has increased greatly during the past decade, but the structural and functional properties of the Sed-Tub fraction remain largely unknown. A proposed model of the effects of glucose on tubulin distribution in human erythrocytes, based on our present and previous findings, is illustrated in Fig. 8. Our *in vivo* and *in vitro* experiments, and analyses of D erythrocytes, suggest that high glucose concentrations induce translocation of tubulin from the Sed-Tub to Mem-Tub fraction, and that such change in tubulin distribution alters deformability and osmotic fragility. More detailed studies of tubulin composition and cellular functions in the future will increase our understanding of the Sed-Tub fraction. The system illustrated in Fig. 8 appears to be a promising target for

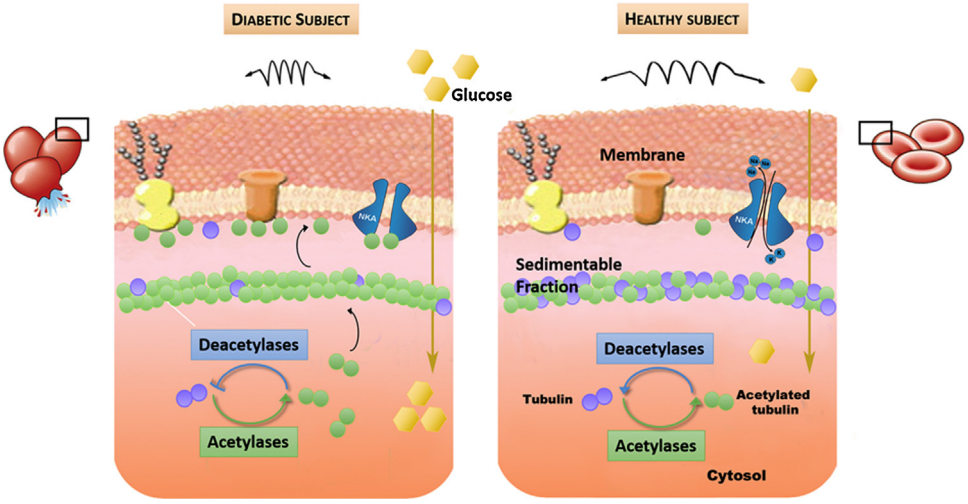

Fig. 8. Proposed model of glucose effects on tubulin distribution, osmotic fragility, and deformability of human erythrocytes. In D erythrocytes, high glucose concentrations promote acetylation of tubulin through inhibition of deacetylases. Glucose also induces translocation of tubulin from the Sed-Tub to Mem-Tub fraction, thereby inhibiting activity of certain enzymes, increasing osmotic fragility, and reducing deformability. In N erythrocytes, tubulin remains localized in the Sed-Tub fraction, and the above membrane-related changes do not occur.

therapy of vascular disorders, including those in advanced diabetes, hypertension, and other metabolic syndrome diseases.

Acknowledgements

This study was supported by grants from the Agencia Nacional de Promoción Científica y Tecnológica de la Secretaría de Ciencia y Tecnología del Ministerio de Cultura y Educación en el marco del Programa de Modernización Tecnológica (PICT 00-00000-01338/08), Consejo Nacional de Investigaciones Científicas y Técnicas (CONICET), Secretaría de Ciencia y Técnica de la Universidad Nacional de Río Cuarto y de la Universidad Nacional de Córdoba, Ministerio de Ciencia y Técnica de la Provincia de Córdoba, Diputación General de Aragón (Grupo Consolidado B20) and European Social Fund (Construyendo Europa desde Aragón). The authors are grateful to Dr. S. Anderson for English editing of the MS.

Appendix A. Supplementary data

Supplementary data associated with this article can be found, in the online version, at http://dx.doi.org/10.1016/j.biocel.2016.02.016.

References

Amaiden, M.R., Santander, V.S., Monesterolo, N.E., Nigra, A.D., Rivelli, J.F., Campetelli, A.N., et al., 2015. Effects of detyrosinated tubulin on Na(+), K(+)-ATPase activity and erythrocyte function in hypertensive subjects. FEBS Lett. 589, 364–373.

Amaiden, M.R., Monesterolo, N.E., Santander, V.S., Campetelli, A.N., Arce, C.A., Pie, J., et al., 2012. Involvement of membrane tubulin in erythrocyte deformability and blood pressure. J. Hypertens. 30, 1414–1422.

Amaiden, M.R., Santander, V.S., Monesterolo, N.E., Campetelli, A.N., Rivelli, J.F., Previtali, G., et al., 2011. Tubulin pools in human erythrocytes: altered distribution in hypertensive patients affects Na+, K+-ATPase activity. Cell. Mol. Life Sci. 68, 1755–1768.

Ariyoshi, K., Maruyama, T., Odashiro, K., Akashi, K., Fujino, T., Uyesaka, N., 2012. Impaired erythrocyte filterability of spontaneously hypertensive rats: investigation by nickel filtration technique. Circ. J. 74, 129–136.

Ballas, S.K., Clark, M.R., Mohandas, N., Colfer, H.F., Caswell, M.S., Bergren, M.O., et al., 1984. Red cell membrane and cation deficiency in Rh null syndrome. Blood 63, 1046–1055.

Behling-Kelly, E., Collins-Cronkright, R., 2014. Increases in beta-lipoproteins in hyperlipidemic and dyslipidemic dogs are associated with increased erythrocyte osmotic fragility. Vet. Clin. Pathol. 43, 405–415.

Berndt-Zipfel, C., Michelson, G., Dworak, M., Mitry, M., Loffler, A., Pfutzner, A., et al., 2013. Vildagliptin in addition to metformin improves retinal blood flow and erythrocyte deformability in patients with type 2 diabetes mellitus—results from an exploratory study. Cardiovasc. Diabetol. 12, 59.

Bradford, M.M., 1976. A rapid and sensitive method for the quantitation of microgram quantities of protein utilizing the principle of protein-dye binding. Anal. Biochem. 72, 248–254.

Cabrales, P., 2007. Effects of erythrocyte flexibility on microvascular perfusion and oxygenation during acute anemia. Am. J. Physiol. Heart Circ. Physiol. 293, 1206–1215.

Campetelli, A.N., Monesterolo, N.E., Previtali, G., Santander, V.S., Amaiden, M.R., Arce, C.A., et al., 2013. Activation of H(+)-ATPase by glucose in Saccharomyces cerevisiae involves a membrane serine protease. Biochim. Biophys. Acta 1830, 3593–3603.

Campetelli, A.N., Previtali, G., Arce, C.A., Barra, H.S., Casale, C.H., 2005. Activation of the plasma membrane H-ATPase of *Saccharomyces cerevisiae* by glucose is mediated by dissociation of the H(+)-ATPase-acetylated tubulin complex. FEBS J. 272, 5742–5752.

Casale, C.H., Previtali, G., Serafino, J.J., Arce, C.A., Barra, H.S., 2005. Regulation of acetylated tubulin/Na+,K+-ATPase interaction by L-glutamate in non-neural cells: involvement of microtubules. Biochim. Biophys. Acta 1721, 185–192.

Casale, C.H., Previtali, G., Barra, H.S., 2003. Involvement of acetylated tubulin in the regulation of Na+,K+ – ATPase activity in cultured astrocytes. FEBS Lett. 534, 115–118.

Casale, C.H., Alonso, A.D., Barra, H.S., 2001. Brain plasma membrane Na+,K+-ATPase is inhibited by acetylated tubulin. Mol. Cell. Biochem. 216, 85–92.

Cohen, W.D., Cohen, M.F., Tyndale-Biscoe, C.H., VandeBerg, J.L., Ralston, G.B., 1990. The cytoskeletal system of mammalian primitive erythrocytes: studies in developing marsupials. Cell Motil. Cytoskeleton 16, 133–145.

Chalkiadaki, A., Guarente, L., 2012. Sirtuins mediate mammalian metabolic responses to nutrient availability. Nat. Rev. Endocrinol. 8, 287–296.

DeWitt, N.D., dos Santos, C.F., Allen, K.E., Slayman, C.W., 1998. Phosphorylation region of the yeast plasma-membrane H+-ATPase. Role in protein folding and biogenesis. J. Biol. Chem. 273, 21744–21751.

Ferru, E., Giger, K., Pantaleo, A., Campanella, E., Grey, J., Ritchie, K., et al., 2011. Regulation of membrane-cytoskeletal interactions by tyrosine phosphorylation of erythrocyte band 3. Blood 117, 5998–6006.

Foller, M., Mahmud, H., Qadri, S.M., Gu, S., Braun, M., Bobbala, D., et al., 2010. Endothelin B receptor stimulation inhibits suicidal erythrocyte death. FASEB J. 24, 3351–3359.

Goodman, S.R., Daescu, O., Kakhniashvili, D.G., Zivanic, M., 2013. The proteomics and interactomics of human erythrocytes. Exp. Biol. Med. (Maywood) 238, 509–518.

Granger, B.L., Repasky, E.A., Lazarides, E., 1982. Synemin and vimentin are components of intermediate filaments in avian erythrocytes. J. Cell Biol. 92, 299–312.

Gundersen, G.G., Kalnoski, M.H., Bulinski, J.C., 1984. Distinct populations of microtubules: tyrosinated and nontyrosinated alpha tubulin are distributed differently in vivo. Cell 38, 779–789.

Gyawali, P., Richards, R.S., 2015. Association of altered hemorheology with oxidative stress and inflammation in metabolic syndrome. Redox Rep. 20, 139–144.

Gyawali, P., Richards, R.S., Hughes, D.L., Tinley, P., 2014. Erythrocyte aggregation and metabolic syndrome. Clin. Hemorheol. Microcirc. 57, 73–83.

Gyawali, P., Richards, R.S., Uba Nwose, E., 2012. Erythrocyte morphology in metabolic syndrome. Expert Rev. Hematol. 5, 523–531.
Hamidi, M., Tajerzadeh, H., Dehpour, A.R., Rouini, M.R., Ejtemaee-Mehr, S., 2001. In vitro characterization of human intact erythrocytes loaded by enalaprilat. Drug Deliv. 8, 223–230.
Kaestner, L., Tabellion, W., Lipp, P., Bernhardt, I., 2004. Prostaglandin E2 activates channel-mediated calcium entry in human erythrocytes: an indication for a blood clot formation supporting process. Thromb. Haemost. 92, 1269–1272.
Karbiner, M.S., Sierra, L., Minahk, C., Fonio, M.C., Bruno, M.P., Jerez, S., 2013. The role of oxidative stress in alterations of hematological parameters and inflammatory markers induced by early hypercholesterolemia. Life Sci. 93, 503–508.
Kosanam, H., Thai, K., Zhang, Y., Advani, A., Connelly, K.A., Diamandis, E.P., et al., 2014. Diabetes induces lysine acetylation of intermediary metabolism enzymes in the kidney. Diabetes 63, 2432–2439.
Koury, S.T., Koury, M.J., Bondurant, M.C., 1989. Cytoskeletal distribution and function during the maturation and enucleation of mammalian erythroblasts. J. Cell Biol. 109, 3005–3013.
Kouzarides, T., 2000. Acetylation: a regulatory modification to rival phosphorylation? EMBO J. 19, 1176–1179.
Kumar, R., 2012. Biochemical changes in erythrocyte membrane in type 2 diabetes mellitus. Indian J. Med. Sci. 66, 131–135.
Laemmli, U.K., 1970. Cleavage of structural proteins during the assembly of the head of bacteriophage T4. Nature 227, 680–685.
Liao, E.C., Paw, B.H., Peters, L.L., Zapata, A., Pratt, S.J., Do, C.P., et al., 2000. Hereditary spherocytosis in zebrafish riesling illustrates evolution of erythroid beta-spectrin structure, and function in red cell morphogenesis and membrane stability. Development 127, 5123–5132.
Lin, C.L., Lee, P.H., Hsu, Y.C., Lei, C.C., Ko, J.Y., Chuang, P.C., et al., 2014. MicroRNA-29a promotion of nephrin acetylation ameliorates hyperglycemia-induced podocyte dysfunction. J. Am. Soc. Nephrol. 25, 1698–1709.
Lin, Y., Berg, A.H., Iyengar, P., Lam, T.K., Giacca, A., Combs, T.P., et al., 2005. The hyperglycemia-induced inflammatory response in adipocytes: the role of reactive oxygen species. J. Biol. Chem. 280, 4617–4626.
Liu, J., Guo, X., Mohandas, N., Chasis, J.A., An, X., 2010. Membrane remodeling during reticulocyte maturation. Blood 115, 2021–2027.
Liu, J., Tang, Y., Feng, Z., Hou, C., Wang, H., Yan, J., et al., 2014. Acetylated FoxO1 mediates high-glucose induced autophagy in H9c2 cardiomyoblasts: regulation by a polyphenol −(−)-epigallocatechin-3-gallate. Metabolism 63, 1314–1323.
Manno, S., Mohandas, N., Takakuwa, Y., 2010. ATP-dependent mechanism protects spectrin against glycation in human erythrocytes. J. Biol. Chem. 285, 33923–33929.
Miller, J.A., Gravallese, E., Bunn, H.F., 1980. Nonenzymatic glycosylation of erythrocyte membrane proteins. Relevance to diabetes. J. Clin. Invest. 65, 896–901.
Mohandas, N., Gallagher, P.G., 2008. Red cell membrane: past, present, and future. Blood 112, 3939–3948.
Monesterolo, N.E., Santander, V.S., Campetelli, A.N., Arce, C.A., Barra, H.S., Casale, C.H., 2008. Activation of PMCA by calmodulin or ethanol in plasma membrane vesicles from rat brain involves dissociation of the acetylated tubulin/PMCA complex. FEBS J. 275, 3567–3579.
Monesterolo, N.E., Nigra, A.D., Campetelli, A.N., Santander, V.S., Rivelli, J.F., Arce, C.A., Casale, C.H., 2015. PMCA activity and membrane tubulin affect deformability of erythrocytes from normal and hypertensive human subjects. Biochim. Biophys. Acta 1848, 2813–2820.
Olearczyk, J.J., Stephenson, A.H., Lonigro, A.J., Sprague, R.S., 2004. NO inhibits signal transduction pathway for ATP release from erythrocytes via its action on heterotrimeric G protein Gi. Am. J. Physiol. Heart Circ. Physiol. 287, H748–H754.
Polevoda, B., Sherman, F., 2002. The diversity of acetylated proteins. Genome Biol. 3, reviews0006.
Rabini, R.A., Petruzzi, E., Staffolani, R., Tesei, M., Fumelli, P., Pazzagli, M., Mazzanti, L., 1997. Diabetes mellitus and subjects' ageing: a study on the ATP content and ATP-related enzyme activities in human erythrocytes. Eur. J. Clin. Invest. 27, 327–332.
Richards, R.S., Nwose, E.U., 2010. Blood viscosity at different stages of diabetes pathogenesis. Br. J. Biomed. Sci. 67, 67–70.
Rivelli, J.F., Amaiden, M.R., Monesterolo, N.E., Previtali, G., Santander, V.S., Fernandez, A., et al., 2012. High glucose levels induce inhibition of Na,K-ATPase via stimulation of aldose reductase, formation of microtubules and formation of an acetylated tubulin/Na,K-ATPase complex. Int. J. Biochem. Cell Biol. 44, 1203–1213.
Santander, V.S., Bisig, C.G., Purro, S.A., Casale, C.H., Arce, C.A., Barra, H.S., 2006. Tubulin must be acetylated in order to form a complex with membrane Na(+), K (+)-ATPase and to inhibit its enzyme activity. Mol. Cell. Biochem. 291, 167–174.
Schwartz, R.S., Madsen, J.W., Rybicki, A.C., Nagel, R.L., 1991. Oxidation of spectrin and deformability defects in diabetic erythrocytes. Diabetes 40, 701–708.
Shin, S., Ku, Y., Babu, N., Singh, M., 2007. Erythrocyte deformability and its variation in diabetes mellitus. Indian J. Exp. Biol. 45, 121–128.
Skalak, R., Hanss, M., Chien, S., 1983. Indices of filterability of red blood cell suspensions. Biorheology 20, 311–316.
Sloboda, R.D., Rosenbaum, J.L., 1982. Purification and assay of microtubule-associated proteins (MAPs). Methods Enzymol. 85 (Pt B), 409–416.
Symeonidis, A., Athanassiou, G., Psiroyannis, A., Kyriazopoulou, V., Kapatais-Zoumbos, K., Missirlis, Y., et al., 2001. Impairment of erythrocyte viscoelasticity is correlated with levels of glycosylated haemoglobin in diabetic patients. Clin. Lab. Haematol. 23, 103–109.
Umudum, F., Yucel, O., Sahin, Y., Bakan, E., 2002. Erythrocyte membrane glycation and NA(+)–K(+) levels in NIDDM. J. Diabetes Complications 16, 359–362.
Uydu, H.A., Yıldırmış, S., Orem, C., Calapoglu, M., Alver, A., Kural, B., Orem, A., 2012. The effects of atorvastatin therapy on rheological characteristics of erythrocyte membrane, serum lipid profile and oxidative status in patients with dyslipidemia. J. Membr. Biol. 245, 697–705.
Xiong, Y., Guan, K.L., 2012. Mechanistic insights into the regulation of metabolic enzymes by acetylation. J. Cell Biol. 198, 155–164.
Zampar, G.G., Chesta, M.E., Carbajal, A., Chanaday, N.L., Diaz, N.M., Casale, C.H., et al., 2009. Acetylated tubulin associates with the fifth cytoplasmic domain of Na(+)/K(+)-ATPase: possible anchorage site of microtubules to the plasma membrane. Biochem. J. 422, 129–137.
Zhao, S., Xu, W., Jiang, W., Yu, W., Lin, Y., Zhang, T., et al., 2010. Regulation of cellular metabolism by protein lysine acetylation. Science 327, 1000–1004.